European Journal of Applied Physiology
https://doi.org/10.1007/s00421-020-04415-4

ORIGINAL ARTICLE

Intra-limb and muscular coordination during walking on slopes

Arthur H. Dewolf[1,2] · **Raphael M. Mesquita**[1] · **Patrick A. Willems**[1]

Received: 15 February 2020 / Accepted: 3 June 2020

Abstract

Purpose Intra-limb and muscular coordination during gait are the result of the organisation of the neuromuscular system, which have been widely studied on a flat terrain. Environmental factors, such as the inclination of the terrain, is a challenge for the postural control system to maintain balance. Therefore, we hypothesised that the central nervous system flexibly modifies its control strategies during locomotion on slopes.

Methods Ten subjects walked on an inclined treadmill at different slopes (from $-9°$ to $+9°$) and speeds (from 0.56 to 2.22 m s^{-1}). Intra-limb coordination was investigated via the Continuous Relative Phase, whereas muscular coordination was investigated by decomposing the coordinated muscle activation profiles into Basic Activation Patterns.

Results A greater stride to stride variability of kinematics was observed during walking on slopes, as compared to walking on the level. On positive slopes, the stride period and width present a greater variability without modification of the time-pattern of the muscular activation and of the variability of intersegmental coordination. On negative slopes, the stride width is larger, the variability of the stride period and of the inter-segmental coordination is greater and the basic activation patterns become broader, especially at slow speeds.

Conclusion Our findings suggest that the control strategy of downhill walking corresponds to a more conservative gait pattern, which could be adopted to lower the risk of falling at the cost of a greater energy consumption. In uphill walking, where metabolic demands are high, the strategy adopted may be planned to minimise energy expenditure.

Keywords Coordination · Neuromuscular control · Basic activation pattern · Continuous relative phase

Abbreviations

CRP	Continuous relative phase
GRF	Ground reaction force
EMG	Records of the electrical activity produced by skeletal muscles
TO	Toe off
COP	Centre of pressure
FC	Foot contact
F_x, F_y, F_z	Lateral, fore-aft and vertical component of the GRF
d_y, d_x	Lateral and fore-aft position of the COP
ω_i, θ_i	Lower-limb segment angular velocity and position
φ_{iN}	Phase angle
ϕ_{iN}	CRP angle
MARP	Mean absolute relative phase
DP	Deviation phase of the CRP
FWHM	Full width at half maximum
CI	Co-activation index
NNMF	Non-negative matrix factorisation
P, W	Basic activation patterns and associated weighting components
VAF	Variability accounted for

Communicated by Lori Ann Vallis.

✉ Arthur H. Dewolf
arthur.dewolf@uclouvain.be

[1] Laboratory of Biomechanics and Physiology of Locomotion, Institute of NeuroScience, Université Catholique de Louvain, Louvain-la-Neuve, Belgium

[2] Department of Systems Medicine and Center of Space Biomedicine, University of Rome Tor Vergata, 00133 Rome, Italy

Introduction

During walking, a high degree of coordination is required to accomplish effective, smooth and accurate movements (Borghese et al. 1996; Chiu and Chou 2012; Winter 1992; Peyré-Tartaruga and Coertjens 2018). Coordination can be defined as the process by which the degrees of freedom are

Published online: 10 June 2020

organised in order to produce a functional movement pattern (Bernstein 1967). For example, lower-limb segment covariation during walking might relate to more global kinematic variables, such as limb length and limb orientation (Dewolf et al. 2018; Ivanenko et al. 2007; Catavitello et al. 2018). Such intra-limb coordination can be investigated by means of the Continuous Relative Phase (CRP). CRP is derived from the angle-velocity phase portrait that contains both spatial and temporal information of two segments (Van Emmerik and Wagenaar, 1996). Furthermore, CRP variability indicates the adaptability of the neuromuscular system to different walking conditions. Large variations are synonymous with decreased stability—defined as the ability to recover from perturbations (Byrne et al. 2002; Chiu and Chou 2012, 2013; Yen et al. 2009).

Such intra-limb coordination depends on the activation of the multiple lower-limb muscles. To simplify the production of movement, the limb muscle activities can be decomposed into a linear combination of a small set of time-dependent commands (so-called the 'basic activation patterns'), the activation of muscles in common patterns (Ivanenko et al. 2004). The number of basic activation patterns recruited to perform a movement and their timing have been linked to the specific ability to perform complex locomotor tasks—such as changing speed (Yokoyama et al. 2016; 2017), cadence (Monaco et al. 2010) or step width (Martino et al. 2015)—in patients with specific mobility impairment—such as stroke patients (Clark et al. 2010; Cheung et al. 2012), children with cerebral palsy (Steele et al. 2015) or with ageing (Allen and Franz 2018). Particularly, fewer and wider basic activation patterns are associated with impaired locomotor coordination and balance control.

Both the intra-limb and muscular coordination underlying human walking have been widely studied on flat terrain. However, on a daily basis, environmental factors, such as the inclination of the terrain, are often encountered and require a modification in the gait pattern. Among others, the slope affects the pendulum-like mechanism of walking (Gottschall and Kram 2006; Gomeñuka et al. 2014, 2016; Dewolf et al. 2017), the lower limb kinematics (Dewolf et al. 2018; Leroux et al. 2002; Prentice et al. 2004), the force and joint moment production (Lay et al. 2006; McIntosh et al. 2006) and muscle activities (Dewolf et al. 2019; Lay et al. 2007; Pickle et al. 2016). These modifications of the gait pattern occur to increase/decrease the potential energy of the body each step but also to ensure stability, especially at slow speeds (Birn-Jeffery and Higham 2014; Dewolf et al. 2018; Hunter et al. 2010; Monsch et al. 2012). The coordination of lower-limb segments and muscle activities while walking on a slope has also been investigated and reveals adaptations in the organisation of the neuromuscular system (Janshen et al. 2017; Rozumalski et al. 2017; Saito et al. 2018), particularly at slow walking speeds (Dewolf et al. 2018, 2019).

These studies show how the central nervous system modifies its control, however only a few explain the reasons of these changes. Hunter et al. (2010) show that, in downhill walking, stability plays a central role in shaping the movement. It is also suggested that the adaptive changes observed both on positive and negative slopes, are aimed to increase gait stability (Ferraro et al. 2013; Vieira et al. 2017) and to reduce the risk of falling (Sheehan and Gottschall 2012).

An optimal neuromuscular control of gait from one stride to the next requires a low stride to stride variability (Hausdorff et al. 2001; Vieira et al. 2017). This moderate variability is a proof of the ability of the central nervous system to cope with unexpected perturbations or errors of execution (Santuz et al. 2018) and contrasts with a rigid unadaptable control system (Cappellini et al. 2016; Martino et al. 2015). An absence of variability will lessen the multiple possible patterns available to negotiate challenging environments. For instance, when toddlers walk on terrains of different inclinations, their adaptability is very limited, and the flexibility of the kinematic pattern is restricted (Dominici et al. 2010). In contrast, a large amount of stride-to-stride variability may be indicative of poor task performance, since subjects are incapable of appropriately selecting a motor strategy from a large number of possibilities to achieve a desired target (Vieira et al. 2017). For instance, a greater variability is correlated with a greater falling risk (Maki 1997), and is thus an indicator of reduced stability (Hausdorff 2007).

Due to the greater instability documented on slopes (Sheehan and Gottschall 2012; Vieira et al. 2017), especially on negative slopes (Hunter et al. 2010; Monsch et al. 2012), we hypothesise that the kinematic inter-stride variability will increase as compared to level walking. In addition, we also hypothesise that the modification of muscular coordination will be similar to the adaption observed during locomotion with challenged stability (Santuz et al. 2018, 2020). In particular, based on the adjustment of motor control strategies when stability is decreased (Martino et al. 2015; Santuz et al. 2018, 2020), we expect a consistent set of neural control elements but a widening of the basic activation patterns.

Methods

Subjects

Data were collected at the same time and on the same subjects as in the study of Dewolf et al. (2017). Six male and four female subjects (22.2 ± 2.4 y.o., mass: 69.2 ± 14.4 kg, height: 1.75 ± 0.10 m, mean ± SD) took part in the study. All subjects were students at the Université catholique de Louvain (UCLouvain, Belgium) and all reported to be in good health. Informed consent was obtained and experimental procedures were performed according the

Declaration of Helsinki and were approved by the Ethics Committee of the Université catholique de Louvain (Ref. No: 2015/06JUL/372).

Procedure and data collection

Subjects were asked to walk on an instrumented treadmill that could be adjusted at four different inclinations (0°, 3°, 6° and 9°). The belt turned forwards to simulate uphill walking or backwards to simulate downhill walking. Six subjects walked on the seven slopes (0°, ± 3°, ± 6°, ± 9°); due to the duration of the experiments, two subjects only walked at 0° and ± 6° and two at 0° and ± 9° out of time constraints. At each slope, half of the subjects started walking uphill and the other half downhill to avoid fatigue bias. Furthermore, the resting period between each trial lasted at least 3′ (> 15′ when the slope of the treadmill had to be changed). Each condition lasted about 2′ from which the last 30″ were recorded. Subjects went through the seven different speeds per slope (between 0.56 and 2.22 m s^{-1}, with an increase of 0.28 m s^{-1} between trials) before moving on to the next slope. At the highest speed, four subjects were spontaneously running, especially on steep slopes and traces were therefore not recorded.

The instrumented treadmill (Arsalis, Belgium) consisted of a modified commercial treadmill (h/p/Comos-Stellar, Germany, belt surface: 1.6 × 0.65 m, mass: ~ 240 kg) combined with four force transducers (as in Dewolf et al. 2016). The force transducers measured the three components of the ground reaction forces (GRF) exerted by the treadmill on the feet.

Kinematic data were recorded at 100 Hz using a high-speed video camera (BASLER A501k, resolution 1280 × 1024 pixels, aperture time: 3 ms) fixed on the ground 3 m to the side of the treadmill, perpendicular to the plane of progression. Fourteen reflective markers were glued on the skin on each side of the subject at the following positions: the chin-neck intersect, the greater trochanter, the lateral femoral condyle, the lateral malleolus, heel and the fifth metatarsophalangeal joint. The final two markers were placed on either side at a point midway between the greater trochanter and the lateral femoral condyle on the lateral side of the thigh, in case the hand hid the hip marker. The horizontal and vertical coordinates of the markers in the sagittal plane were measured in each frame. A spline function was fitted through the coordinate data, sampled at 100 Hz, to smoothen and interpolate the signal to 1000 Hz [as in (Gambelli et al. 2016)].

Electromyographic (EMG) activities from 16 muscles on the right side of each subject were recorded at 2 kHz using a Delsys Trigno Wireless System (Boston, MA): *erector spinae* (ES) at L2 level, *gluteus maximus* (Gm), *gluteus medius* (Gmed), *sartorius* (SART), *tensor fasciae latae* (TFL), *adductor longus* (ADD), *vastus medialis* (VM), *vastus lateralis* (VL), *rectus femoris* (RF), long head of the *biceps femoris,* (BF), *semitendinosus* (ST), *tibialis anterior* (TA), *medial gastrocnemius* (MG), *lateral gastrocnemius* (LG), *soleus* (SOL) and *peroneus longus* (PERL). After preparing the abraded shaved skin with ether and alcohol, EMG electrodes were placed based on suggestions from SENIAM (seniam.org), the European project on surface EMG. To ensure correct placement of EMG electrodes, muscle bellies were located by means of palpation and the electrodes were oriented along the main direction of the fibres (Kendall et al. 2005; Winter 1991). We verified electrode position and signal quality by visually inspecting the EMG signals while subjects contracted each instrumented muscle. In certain conditions, some electrodes became partially detached and were removed on a subject-specific basis. The average number of muscle EMG traces from each subject in each condition was 15.3. Acquisition of the EMG, kinematic, and kinetic data was synchronised.

Data analysis

Division of stride

The stride period was defined as the time between two successive right foot contacts (FC). FC and toe off (TO) were estimated from the displacement of the centre of pressure (COP) on the belt. The lateral (d_y) and fore-aft (d_x) position of the COP was computed from the GRFs using the procedure described in Dewolf et al. (2018):

$$d_x = \frac{-M_y - hF_x}{F_z}, \tag{1}$$

$$d_y = \frac{-M_x - hF_y}{F_z}, \tag{2}$$

where F_x, F_y and F_z are the lateral, fore-aft and vertical GRFs, respectively; M_x and M_y the moment components in the force transducer coordinate system; and h is the vertical distance between the force transducers and the tread-surface (Xu et al. 2015). The stride width was then defined as max (d_y) − min (d_y) over a stride. We also assessed the inter-stride variability by calculating the mean standard deviation (SD) of the stride period.

Kinematics

From marker locations, the orientation of the thigh, shank and foot relative to the vertical axis (elevation angle) were computed as described in Borghese et al. (1996). For each subject, elevation angles were truncated on a stride-by-stride basis and interpolated to 400 points across the time

of each complete gait cycle (i.e. every 0.25% of the stride). The inter-stride angular variability was assessed by calculating the mean standard deviation of the thigh, shank and foot elevation angles.

Intra-limb coordination was assessed by using the Continuous Relative Phase (CRP) technique (Ogaya et al. 2016; Ranavolo et al. 2013; Yen et al. 2009). A custom-written Labview (National instruments, Inc.) program was used to calculate the CRP values as described hereafter. For each of the 400 interpolated data points within a gait cycle, the lower-limb segment angular velocities (ω_i) and positions (θ_i) were first normalised on a stride-per-stride basis. In order to fit the normalised values between −1 and +1, ω_{iN} and θ_{iN} were computed as followed:

$$\omega_{iN} = \frac{\omega_i}{\max\left(|\omega_i|\right)}, \tag{3}$$

$$\theta_{iN} = 2\left(\frac{\theta_i - \min\left(\theta_i\right)}{\max\left(\theta_i\right) - \min\left(\theta_i\right)}\right) - 1, \tag{4}$$

where $i = [1{:}400]$. The phase portrait of each lower-limb segment elevation angle was generated by plotting its normalised angular velocity (ω_{iN}) against its normalised angular position (θ_{iN}). Once the phase portrait was obtained, the phase angle (φ_{iN}) was calculated as:

$$\varphi_{iN} = \tan^{-1}\frac{\omega_{iN}}{\theta_{iN}}. \tag{5}$$

The CRP angle (ϕ_{iN}) between each pair of lower-limb segments was then computed by subtracting the value of the phase angle of the distal segment from that of the proximal segment ($\phi_{i,\text{thigh}-\text{shank}} = \varphi_{i,\text{thigh}} - \varphi_{i,\text{shank}}$ and $\phi_{i,\text{shank}-\text{foot}} = \varphi_{i,\text{shank}} - \varphi_{i,\text{foot}}$). The intra-limb coordination and its variability were then assessed by measuring the mean absolute relative phase (MARP) and the deviation phase (DP). $\text{MARP}_{\text{thigh-shank}}$ and $\text{MARP}_{\text{shank-foot}}$ were computed by averaging over the stride the absolute values of $\phi_{i,\text{thigh}-\text{shank}}$ and $\phi_{i,\text{shank - foot}}$ respectively, whereas $\text{DP}_{\text{thigh-shank}}$ and $\text{DP}_{\text{shank-foot}}$ were calculated by averaging the corresponding standard deviations. MARP provides a measure of intra-limb coordination: a low MARP indicates that the movements of adjacent segments are in-phase while a greater MARP indicates that the movements become more out-of-phase and behave in a less similar manner. DP represents the stride-to-stride variability and provides a measure of stability in the organisation of the neuromuscular system: a low DP indicates a more rigid coordination between two adjacent segments (Stergiou et al. 2001).

Assessment of EMGs

The raw EMG signals were high-pass filtered (30 Hz), then rectified and low-pass filtered with a zero-lag third-order Butterworth filter (10 Hz). To reduce residual baseline noise, which appears as offsets in the EMG envelopes, we subtracted the minimum signal from each EMG. The time scale was normalised by interpolating individual gait cycles over 400 points. For each individual, the EMG signal from each muscle was normalised to its peak value across all trials.

For each condition and for each EMG waveform, the full width at half maximum (FWHM) was calculated as the duration during which the EMG activity exceeded the half of its maximum (Martino et al. 2014). The mean FWHM was also calculated by averaging the FWHM of the 16 muscles studied.

We also assessed a co-activation index (CI) between the antagonistic muscle groups at the level of the thigh (quadriceps vs hamstring) and of the shank (triceps vs TA). Therefore, the mean activity of the quadriceps was assessed at each instant by averaging the EMG amplitudes of the RF-VL-VM muscles, that of the hamstring by averaging BF-ST and that of the triceps by averaging SOL-MG-LG. For each of the 400 points of the gait cycle, the highest activity between the quadriceps and the hamstring muscles (or between triceps and TA) is defined as $\text{EMG}_{i\text{H}}$ and accordingly, the lowest activity as $\text{EMG}_{i\text{L}}$. The co-activation indexes (CI) at the level of the thigh or the shank were then computed over the stride as follows (Mari et al. 2014; Martino et al. 2014):

$$\text{CI} = \frac{\sum_{i=1}^{400}\left(\left[\text{EMG}_{i\text{H}} + \text{EMG}_{i\text{L}}\right]/2\right) \times \left(\text{EMG}_{i\text{L}}/\text{EMG}_{i\text{H}}\right)}{400}. \tag{6}$$

A small CI represents a low level of co-activation (Rudolph et al. 2000).

Basic activation patterns

Basic activation patterns are component factors that can account for a considerable fraction of the total EMG pattern variance in a large number of muscles active during locomotion (Ivanenko et al. 2004). These basic patterns were extracted using the non-negative matrix factorisation (NNMF) algorithm. For every subject, slope and speed, the average muscle excitations normalised to its peak value across all trials were concatenated into an $m \times n$ matrix (M), where m indicates the number of muscles and n is the number of time- normalised samples (400). The NNMF algorithm was applied to M in order to identify the underlying basic activation patterns P and associated weighting components W (Lee and Seung 2001), as follows:

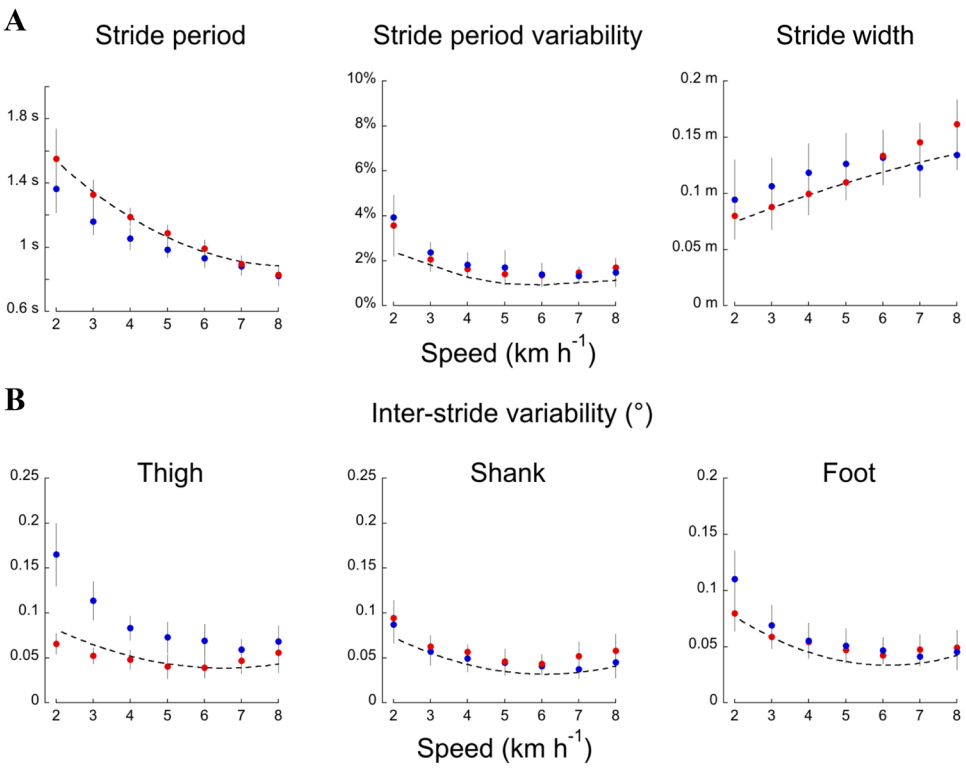

Fig. 1 **a** Stride period (left), stride period variability (middle) and step width (right) during walking on a + 9° positive slope (red symbols) and − 9° downhill slope (blue symbols) as a function of speed. **b** Inter-stride variability of the thigh (left), shank (middle) and foot (right) elevation angles during walking on a + 9° positive slope (red symbols) and − 9° downhill slope (blue symbols) as a function of speed. In each panel, interrupted lines correspond to the data obtained during level walking and symbols and bars represent the grand means and SDs of all subjects (SDs are presented only when the length of the bar exceeds the size of the symbol). The interrupted lines were drawn through experimental data using a weighted mean function (KaleidaGraph 4.5; Synergy Software, USA)

$$M = P \times W + e, \tag{7}$$

where e is the residual error matrix. The algorithm searches for an approximate solution to minimise the root-mean-squared error between M and $P \times W$. For a given number of motor components (see below), the factorisation uses an iterative method starting from randomly chosen initial conditions for P and W (Gizzi et al. 2011; Ivanenko et al. 2005; Sartori et al. 2013). Because the root-mean-squared error may have local minima, the best solution was selected out of 100 runs to find W and P from multiple random starting values. The goodness of the pattern decomposition was assessed with the percent of variability accounted for index (VAF; Torres-Oviedo et al. 2006), defined as:

$$\mathrm{VAF} = 1 - \frac{\mathrm{SSE}}{\mathrm{TSS}}, \tag{8}$$

where SSE is the sum of squared errors between the experimental and reconstructed excitations and TSS is the total sum of squares (Dominici et al. 2011; Ivanenko et al. 2006; Sartori et al. 2013). To determine the minimum number of basic activity patterns which best accounts for the EMG data variance, we iterated analyses by varying the number of synergies between 1 and 8. Four motor modules were assumed for each condition (as in previous study, e.g. Dominici et al. 2011; Dewolf et al. 2019; Baggen et al. 2020) because it accounted for > 90% of total variance (Torres-Oviedo and Ting 2007; Saito et al. 2018) and adding an additional component increased VAF by < 5% (see results). This double criterion approach was selected in order to adequately reproduce relevant features of the synergy compositions.

To compare spatio-temporal characteristics, individual synergies obtained from different subjects were pooled and matched based on the correlation of their structure (W) using a custom cluster analysis algorithm. In brief, each pattern was ordered based on the degree of similarity across subjects, which was evaluated based on the best-matching scalar product of weighting coefficient normalised to Euclidean norm (Cheung et al. 2005; Dewolf et al. 2019; Martino et al. 2015). For each basic activation pattern, the peak value and the full width at half maximum (FWHM) was calculated as the period during which the EMG activity exceeded the half of its maximum (Martino et al. 2015). In addition, similarities of the associated weighting coefficient between level and slope walking at each speed of progression were assessed by measuring the scalar product between data of individual subjects walking on slope and its data walking on the level at matched speed.

Statistics

Data were grouped into speed-slope classes. To obtain one value per subject in each class, all strides of a subject in a given class were averaged. The mean and standard deviation of the population were then computed in each class (grand mean). The statistical analysis was designed to assess the

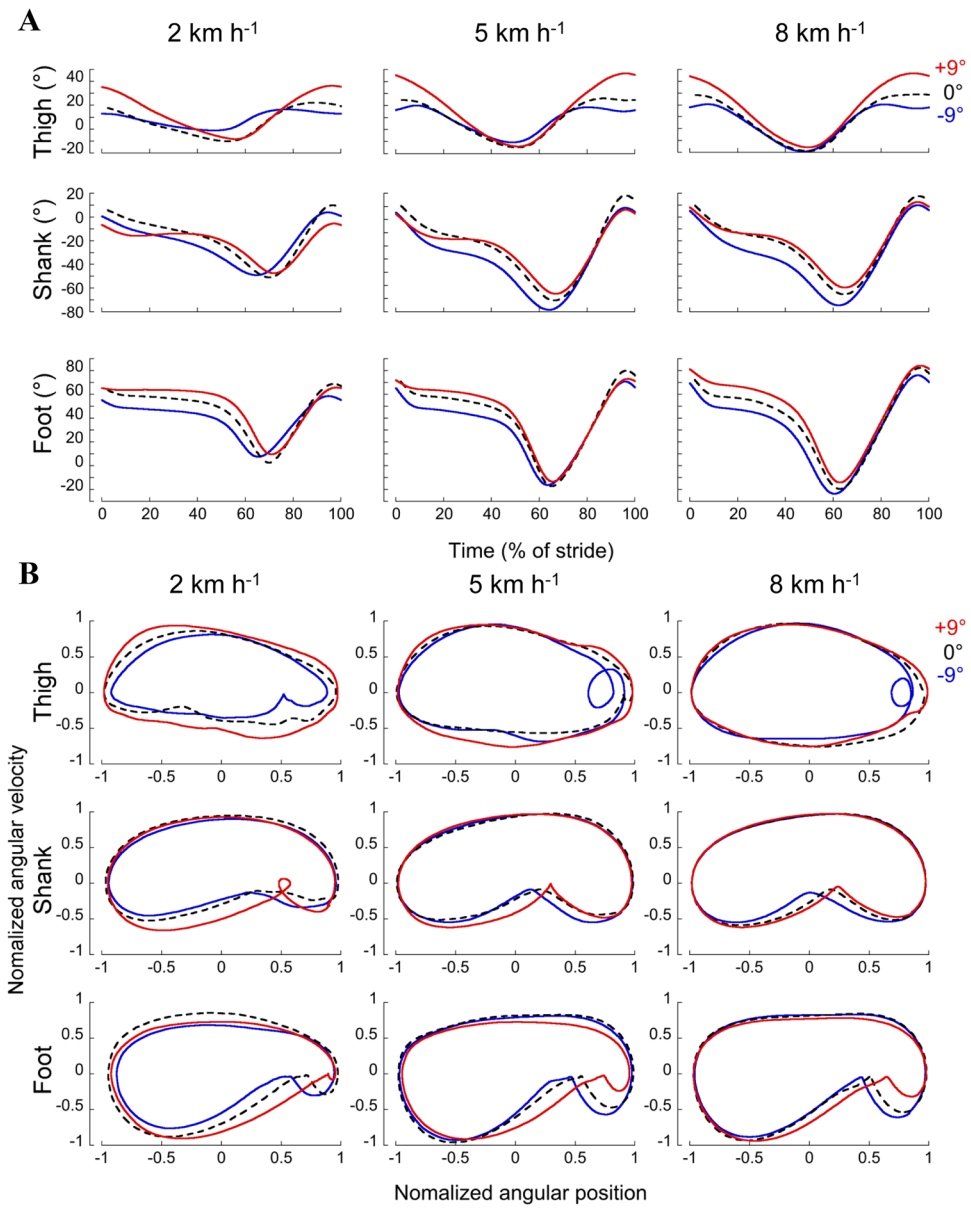

Fig. 2 **a** Thigh (top), shank (middle), and foot (bottom) elevation angles as a function of time during walking at 0.56 m s^{-1} (left), 1.39 m s^{-1} (middle) and 2.22 m s^{-1} (right) on a −9° downhill slope (blue lines), on the level (interrupted lines) and on a +9° uphill slope (red lines). Time is expressed in percent of the stride period: 0% and 100% correspond to the right-foot contact. **b** Normalised phase portrait of the thigh (top), shank (middle), and foot (bottom) elevation angles over a stride during walking at 0.56 m s^{-1} (left), 1.39 m s^{-1} (middle) and 2.22 m s^{-1} (right) on a -9° downhill slope (blue lines), on the level (interrupted lines) and on a +9° uphill slope (red lines)

effect of speed, slope and of the interaction between these two factors. A two-level linear mixed model ANOVA with post-hoc *Bonferroni* correction (PASW Statistics 19, SPSS inc®, IBM company, USA) was applied: speed and slope were set as fixed effects, and the subject was set as a random effect. The normality of the residuals was checked visually with QQ-plots. Normality of the residuals was not assumed for 4 variables (stride period variability, thigh and shank inter-stride variability and ES FWHM). In those cases, an inverse transformation was applied and the normality of the residuals was then assumed. A α-threshold of 0.05 was used throughout to assess statistical significance.

Results

General gait parameters

A two-level linear mixed model ANOVA has been conducted to examine the effect of slope and speed on the stride period, the stride period variability and the stride width (Fig. 1a). No statistically significant interaction between the effects of slope and speed is found on the stride period ($F = 23.9$; $p = 0.08$), on the stride period variability ($F = 1.8$; $p = 0.06$) or on the stride width ($F = 1.2$; $p = 0.321$).

Simple main effect analysis reveals that (1) at all slopes, the stride period is significantly smaller as speed increases ($F = 71.1$; $p < 0.001$) and (2) as compared to level walking the stride period is significantly reduced when walking

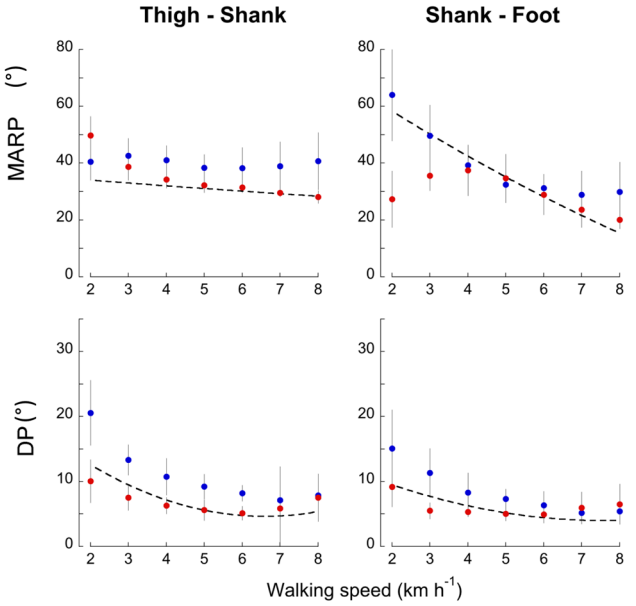

Fig. 3 Mean absolute relative phase, MARP (upper panels) and the deviation phase, DP (bottom panels) of the thigh-shank (left panels) and shank-foot (right panels) segment-coordination during walking on a +9° positive slope (red symbols) and −9° downhill slope (blue symbols) as a function of speed. In each panel, interrupted lines correspond to the data obtained during level walking. Other indications as in Fig. 1

downhill ($F=19.3$; $p<0.001$). Furthermore, both speed and slope affect stride period variability ($F=19.1$; $p<0.001$ and $F=117.7$; $p<0.001$, respectively). *Bonferroni* post-hoc reveals that the stride period variability is significantly greater when walking on a +9° or −9° slope, as compared to the level ($p<0.001$ for −9° & +9°). Speed and slope also affect stride width ($F=8.2$; $p<0.001$ and $F=56.3$; $p<0.001$, respectively). *Bonferroni* post-hoc reveals that the stride width is significantly greater when walking on a +9° or −9° slope, as compared to the level ($p<0.001$ for −9° and +9°).

Intra-limb coordination and its variability

The mean curves of thigh shank and foot elevation angles and phase portrait at 3 different speeds and at −9°, 0° and +9° are presented in Fig. 2a and B. A two-level linear mixed model ANOVA has been conducted to examine the effect of slope and speed on inter-stride variability of thigh, shank and foot elevation angles, on MARP and DP of $\phi_{i,\text{thigh}-\text{shank}}$ and $\phi_{i,\text{shank}-\text{foot}}$ (Fig. 3). No statistically significant interaction between the effects of speed and slope is found on inter-variability of thigh, shank and foot elevation angles ($F=0.7$; $p=0.841$, $F=0.8$; $p=0.700$ and $F=0.9$; $p=0.586$, respectively). Simple main effect analysis reveals that thigh, shank and foot inter-stride variability are reduced with increasing speed ($F=59.8$; $p<0.001$ for thigh, $F=71.6$; $p<0.001$ for shank and $F=26.1$; $p<0.001$ for foot). The slope of the terrain also affects the inter-stride variability ($F=38.3$; $p<0.001$ for thigh, $F=10.6$; $p<0.001$ for shank and $F=4.3$; $p=0.002$ for foot). As compared to the level, *Bonferroni* post-hoc reveals that (1) the thigh inter-variability is significantly greater when walking on a -6° and -9° slope ($p<0.001$ on both slopes), (2) shank variability is increased on a +6° and +9° slope ($p=0.001$ on both slopes) and (3) foot variability is significantly greater when walking on a -9° slope, as compared to the level ($p=0.001$).

A statistically significant interaction between the effects of slope and speed is found on $\text{MARP}_{\text{thigh-shank}}$ and $\text{MARP}_{\text{shank-foot}}$ ($F=1.7$; $p=0.08$ and $F=6.3$; $p<0.001$). Simple main effect analysis reveals that both $\text{MARP}_{\text{thigh-shank}}$ and $\text{MARP}_{\text{shank-foot}}$ decrease with increasing speed ($F=23.0$; $p<0.001$ and $F=128.3$; $p<0.001$, respectively). In addition, $\text{MARP}_{\text{thigh-shank}}$ and $\text{MARP}_{\text{shank-foot}}$ are also affected by slope ($F=39.8$; $p<0.001$ and $F=28.6$; $p<0.001$, respectively): as compared to the level, at slow speeds $\text{MARP}_{\text{thigh-shank}}$ is greater on negative slopes whereas at fast speeds, $\text{MARP}_{\text{thigh-shank}}$ is greater on positive slopes. The major difference in $\text{MARP}_{\text{shank-foot}}$ occurs at slow speeds on positive slopes.

No statistically significant interaction between the effects of slope and speed is found on $\text{DP}_{\text{thigh-shank}}$ and $\text{DP}_{\text{shank-foot}}$ ($F=1.7$; $p=0.08$ and $F=1.4$; $p=0.169$). Simple main effect analysis reveals that $\text{DP}_{\text{thigh-shank}}$ and $\text{DP}_{\text{shank-foot}}$ decrease with increasing speed ($F=45.4$; $p<0.001$ and $F=31.0$; $p<0.001$, respectively). In addition, $\text{DP}_{\text{thigh-shank}}$ and $\text{DP}_{\text{shank-foot}}$ are also affected by slope ($F=16.1$; $p<0.001$ and $F=6.7$; $p<0.001$, respectively). *Bonferroni* post-hoc reveals that both $\text{DP}_{\text{thigh-shank}}$ and $\text{DP}_{\text{shank-foot}}$ are significantly greater when walking on a -6° and -9° slope as compared to the level ($p<0.006$).

The coordination of muscular activity

Typical traces of the 16 raw EMG data are presented in Fig. 4. A two-level linear mixed model ANOVA has been conducted to examine the effect of slope and speed on the average and individual FWHM of lower-limb muscles and on CI between the thigh and shank (Fig. 5). The FWHM of all lower-limb muscles except the ADD and BF decreases with speed of progression ($F>3.6$; $p<0.02$). The slope of the terrain also affects the FWHM: as compared to the level, *Bonferroni* post-hoc reveals that ES, GM, RF, MG, LG, SOL and PERL have a greater FWHM in −9° downhill walking whereas Gmed, TFL and ST have a greater FWHM in +9° uphill walking. The mean FWHM across 16 lower-limb muscles is reduced with the speed of progression ($F=79.1$; $p<0.001$) from 30.8% at 0.56 m s^{-1} to 19.5% at 2.22 m s^{-1}.

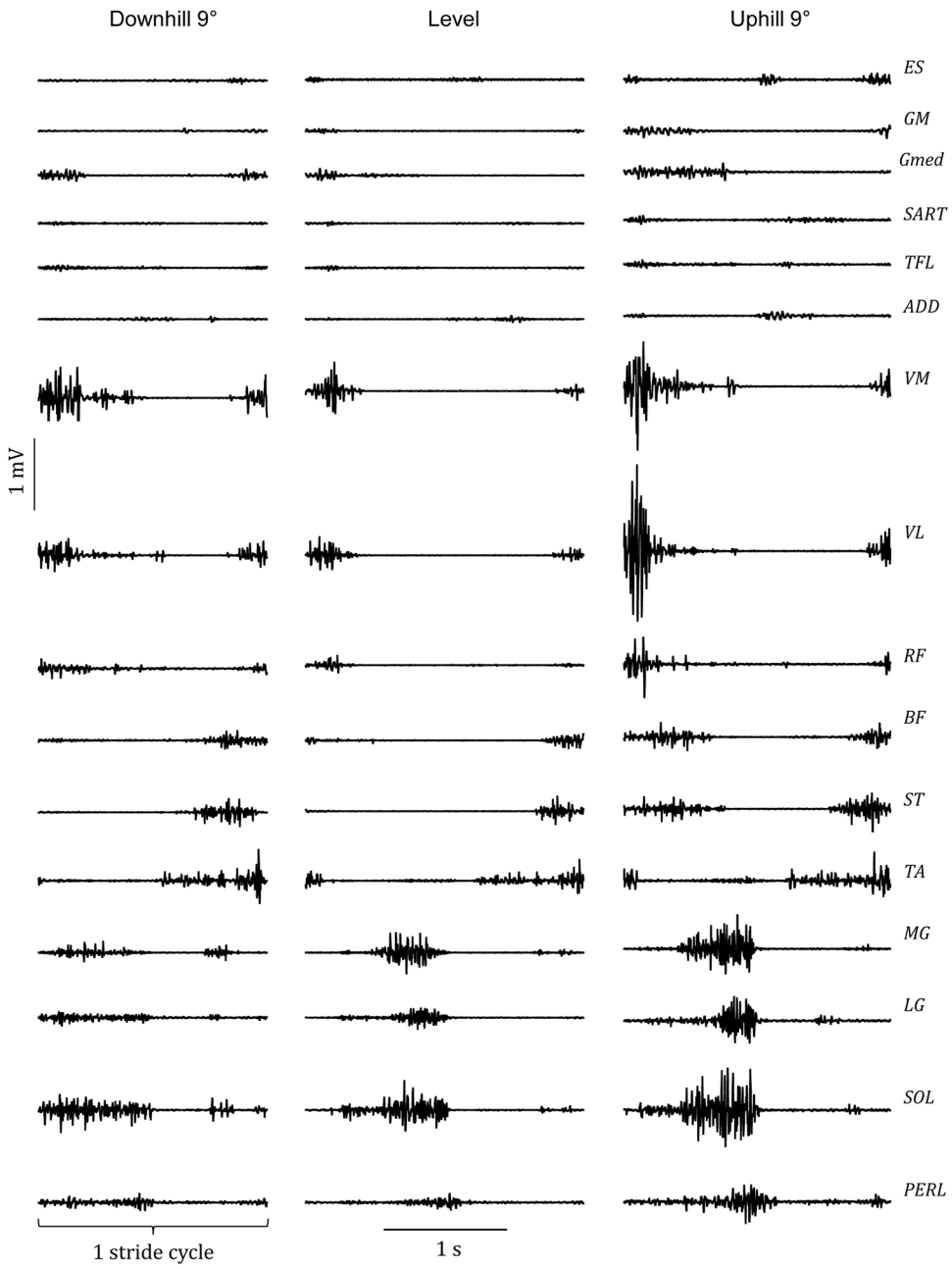

Fig. 4 Raw EMG patterns of 16 lower-limb muscles during one stride of walking at ~ 1.39 m s^{-1} on a −9° downhill slope (left), on the level (middle) and on a +9° uphill slope (right). From top to bottom, *ES* is for *erector spinae*, *GM gluteus maximus*, *Gmed gluteus medius*, *SART sartorius*, *TFL tensor fascia latae*, *ADDL adductor longus*, *VM vastus medialis*, *VL vastus lateralis*, *RF rectus femoris*, *BF biceps femoris*, *ST semi tendinous*, *TA tibialis anterior*, *GM gastrocnemius medialis*, *LG lateral gastrocnemius*, *SOL soleus*, *PERL peroneus longus*

The average FWHM also differs with the slope: as compared to the level, FWHM is increased when walking on a − 9° slope (27.1% vs. 21.7%; $p < 0.001$) whereas the mean FWHM is not affected on a +9° slope (21.7% vs. 21.5%; $p = 0.99$).

No statistically significant interaction between the effects of slope and speed is found on the CI of both the thigh and the shank muscles ($F = 0.4$; $p = 0.988$ and $F = 0.9$; $p = 0.568$). Simple main effect analysis reveals that the CI of the thigh and of the shank muscles decreases with increasing speed ($F = 28.5$; $p < 0.001$ and $F = 35.3$; $p < 0.001$, respectively). In addition, both CIs are also affected by slope ($F = 16.8$; $p < 0.001$ and $F = 12.1$; $p < 0.001$, respectively): *Bonferroni* post-hoc reveals that the two CIs are significantly greater when walking on a positive +9° slope, as compared to walking on the level ($p < 0.001$).

Analysis of dimensionality with the NNMF method shows that the EMG activity changes during slope walking are captured by a small number of motor modules (Fig. 6). The total VAF percentage by four basic patterns is equal to 92.4 ± 1.6% and adding an additional component only increased VAF by 3.43 ± 0.37%.The average basic activation patterns and the associated weighting coefficients are presented across slopes at three different speeds (Fig. 6a). The

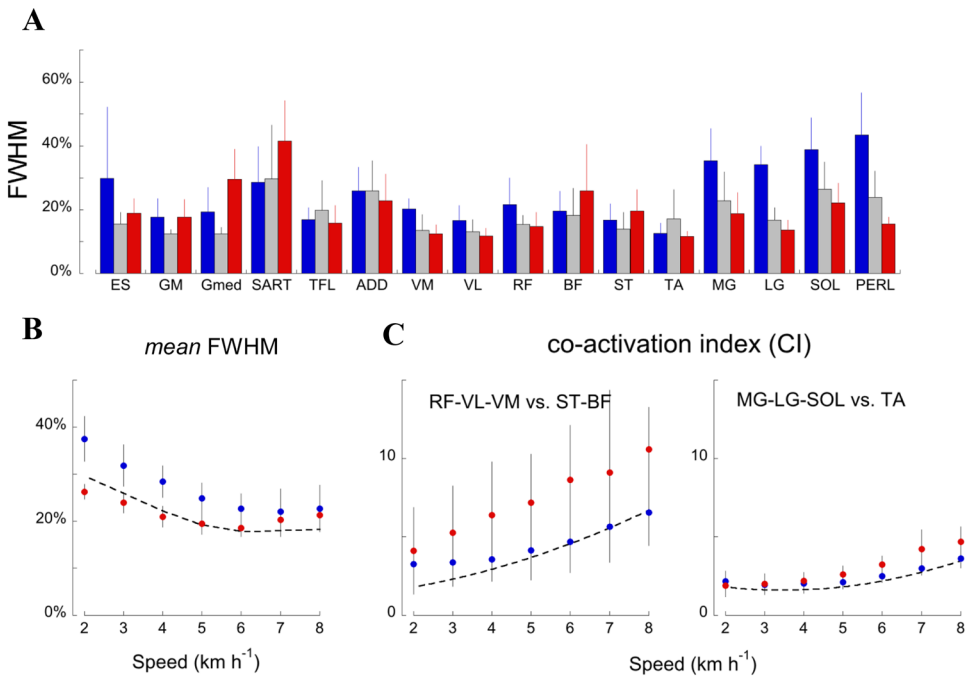

Fig. 5 **a** Full Width Half Maximum (FWMH) of the 16 lower-limb muscles during walking at ~ 1.39 m s^{-1} on a −9° downhill slope (blue), on the level (grey) and on a +9° uphill slope (red). Symbol of the muscles as in Fig. 4. **b** The mean FWHM across the 16 lower-limb muscles during walking on a −9° slope (blue), on the level (grey) and on a +9° slope (red) as a function of speed. **c** Co-activation index (see methods) between knee flexor and extensor (left) and between ankle flexor and extensor (right) as a function of speed. In **b** and **c**, interrupted lines correspond to the data obtained during level walking. Other indication as in Fig. 1

muscle weightings are generally similar between conditions as compared to level (scalar product mean ± SD 0.74 ± 0.24). However, significant effects of speed and slope are observed (Fig. 6a): the similarities with level walking are greater at fast walking speeds ($F = 3.97$; $p = 0.029$) and on positive than on negative slopes ($F = 4.83$; $p = 0.033$).

The timing of activity peaks (Fig. 3b) is relatively invariant across speeds and slopes. However, the amplitude of the basic activation patterns are modified with speed and slope. The peak value of the four basic activation patterns increases with speed of progression ($F = 348.9$; $p < 0.001$) from −9° to +9° ($F = 106.9$; $p < 0.001$). In particular, the slope mainly affects the magnitude of the second pattern (interaction: $F = 13.2$; $p < 0.001$), occurring at the end of the stance and corresponding to the propulsion phase (Ivanenko et al. 2004; Dewolf et al. 2019): its peak decreases in downhill walking and increases in uphill walking, as compared to the level (0.29 ± 0.51% at −9° vs. 0.516 ± 0.02% at 0° vs. 0.70 ± 0.02% at +9°; $p < 0.001$).

A two-level linear mixed model ANOVA has been conducted to examine the effect of slope and speed on the VAF and on the mean FWHM of the four basic activation patterns (Fig. 6b). No statistically significant interaction between the effects of slope and speed is found on VAF and FWHM of the basic activation patterns ($F = 0.9$; $p = 0.520$ and $F = 1.2$; $p = 0.341$). The VAF of the four basic activation patterns slightly decreases with speed of progression ($F = 9.5$; $p < 0.001$). The slope of the terrain also affects the VAF ($F = 9.6$; $p < 0.001$): in particular, the variance accounted for only one basic pattern is much greater in downhill walking as compared to the level (27 ± 1.2% in level walking vs. 55.6 ± 1.4% in downhill walking; $p < 0.001$).

The average FWHM across the four basic activation patterns is reduced with the speed of progression ($F = 40.7$; $p < 0.001$) from 22.3% at 0.56 m s^{-1} to 15.9% at 2.22 m s^{-1}. The mean FWHM also differs with the slope: as compared to the level, FWHM is increased in downhill walking (17.0 ± 0.4% on the level vs. 19.1 ± 0.4% at −6° and 20.4 ± 0.5% at −9°; $p < 0.001$) whereas positive slopes do not affect significantly the mean FWHM (17.0 ± 0.4% on the level vs. 18.9 ± 0.5% at +9°; $p = 0.058$).

Discussion

The present study examines the intra-limb and muscular coordination of walking on different slopes and at various speeds. Our results show modifications of general gait parameters, intra-limb coordination and EMG activity when walking on a slope. These observations support our hypothesis that the adjustment of motor control strategies on slopes, suggesting a more challenging task for the neuromuscular control, are similar to those observed during locomotion with a reduction of stability (Martino et al. 2015; Allen and Franz 2018; Santuz et al. 2018, 2020).

When gait stability is confronted with an irregular terrain or even with a virtual environment, strides become shorter and wider as the perturbation intensity increases (Hak et al. 2012; Santuz et al. 2018). Similar adaptive changes of stride length and width have been observed in patients with known balance disorders, such as patients with cerebellar ataxia

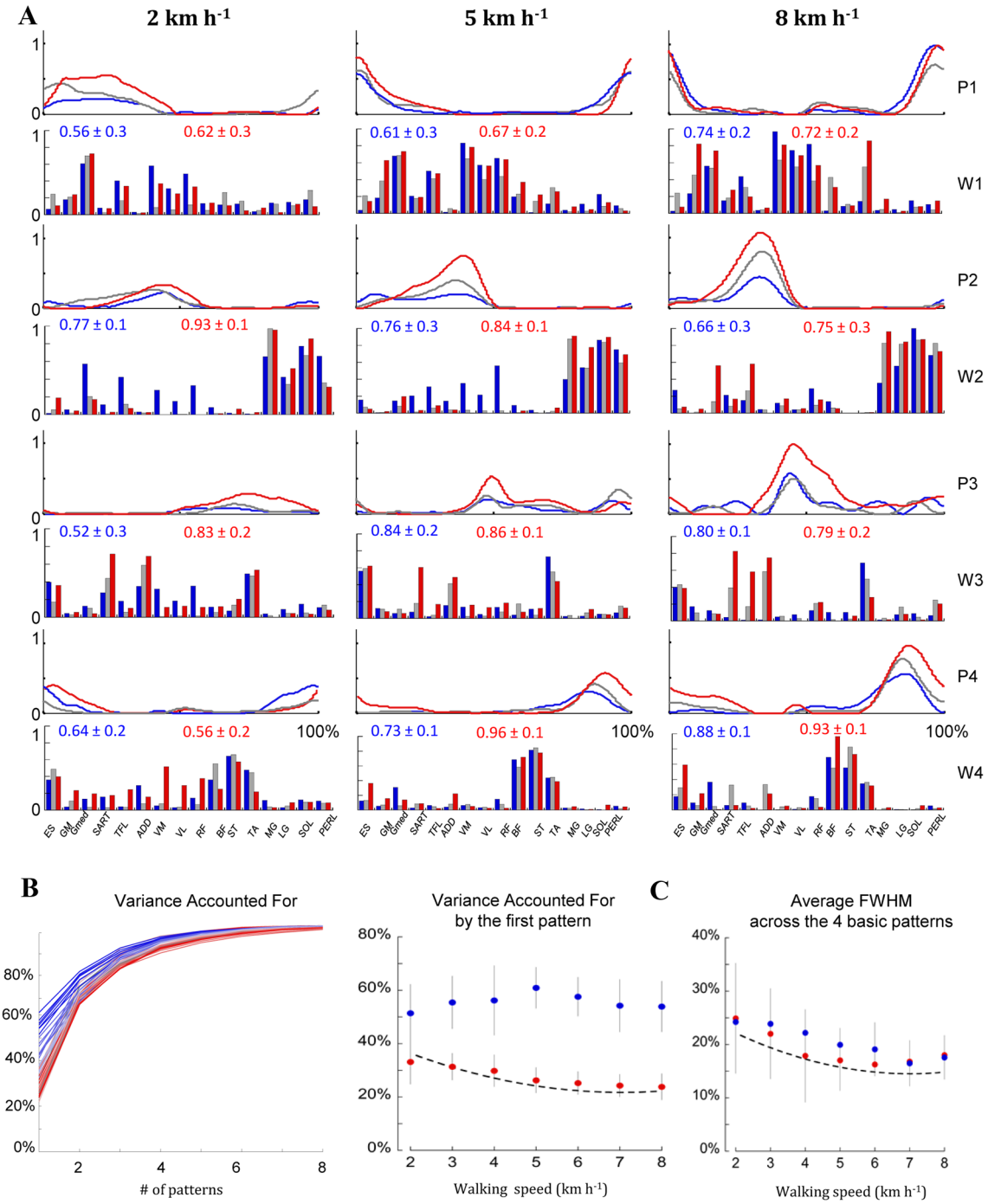

(Martino et al. 2015). Indeed, ataxic patients have a reduced stride length and a larger stride width than healthy adults. When walking on a slope, strides become wider than on a flat terrain (Fig. 1a). Furthermore, on negative slopes, strides become shorter (Fig. 1a and McIntosh et al. 2006). These observations suggest that the adaptations of gait parameters are similar to the strategy adopted to ensure gait stability.

Walking on uneven surfaces or with perturbations of balance has also been associated with greater gait variability (McAndrew et al. 2010; Santuz et al. 2018). As observed, the inter-stride period variability increased on slopes which is in accordance with the higher trunk acceleration variability in inclined terrains (Vieira et al. 2017), an indicator of poorer task performance that also seems to play a role to explain the higher metabolic cost (Rosa et al. 2018). Indeed, greater variability has been suggested to be detrimental to system performance. For example, Hunter et al. (2010) show that, in downhill walking, ensuring gait stability is done at

◂**Fig. 6** **A:** The panels on the lines labelled P_i present the basic activation patterns as a function of time during walking at 0.83, 1.39 and 1.94 m s^{-1} on different slopes (negative slopes: toned-down blue colours, positive slopes: toned-down red colours). Time is expressed relative to the stride period: 0% and 100% correspond the right foot contact. The panels on the lines labelled W_i present the corresponding group mean weights assessed using non-negative matrix factorisation. The basic activation patterns are labelled in a "chronological" order: P1–W1 appears around foot contact, P2–W2 corresponds roughly at the end of single stance, P3–W3 occurs roughly during double contact and at the beginning of swing phase and P4–W4 at the end of swing phase. Each curve represents the ensemble-averaged pattern for a specific slope. The numbers on the top of each plot represent the mean scalar product of weights of individual subjects at −9° (blue) and +9° (red) with individual subjects on the level. **b** Cumulative percent of variance (VAF) explained by the *n* first basic EMG patterns at all speeds and slopes (left). Negative slopes correspond to toned-down blue colours and positive slopes correspond to toned-down red colours. VAF if the number of patterns is constraint to one (right) during walking on a +9° positive slope (red) and −9° downhill slope (blue) as a function of speed. **c** Average Full width half maximum (FWHM) across the four basic patterns during walking on a −9° downhill slope (blue) and on a +9° uphill slope (red) as a function of speed. In **b** and **c**, interrupted lines correspond to the data obtained during level walking and symbols and bars represent the grand means and SDs of all subjects (SDs are presented only when the length of the bar exceeds the size of the symbol)

the expense of walking economy. Indeed, subjects adopt a more conservative gait strategy: they walk with decreased stride periods and stride lengths, increased metabolic rate and demonstrated a greater stride to stride variability and modify the nonlinear dynamics of gait (Monsch et al. 2012). The adaptations in stride length, width and variability have also been associated with increased risk of falls (Maki 1997). This last author shows that individuals with higher variability and wider step width experienced a greater number of falls. Even though variability is a necessary characteristic in adaptability, our results suggest that inclined terrain increases gait variability (Sheehan and Gottschall 2012; Vieira et al. 2017).

From a kinematic point of view, the control of gait coordination was investigated by means of the CRP technique. The choice of such method instead of others based on principal component analysis (e.g. Borghese et al. 1996; Noble and Prentice 2008) was done so to quantify the variability (DP) of the coupling relationship between two adjacent segments. Our findings suggest that adjustments to speed changes are mainly accomplished by changing the $MARP_{shank\text{-}foot}$ and to a lesser extent the $MARP_{thigh\text{-}shank}$. A smaller MARP indicates a more in-phase behaviour of the inter-segmental relationships. This is in accordance with Bianchi et al. (1998), Grasso et al. (2000) and Dewolf et al. (2018), who showed that the phase shift of the shank angle relative to the thigh angle and that of the foot angle relative to the shank angle decreases with increasing speed. The adjustments of CRP to slope are mostly accomplished by changing the $MARP_{thigh\text{-}shank}$ in downhill walking and by changing the $MARP_{shank\text{-}foot}$ in uphill walking. Indeed, as compared to level walking, the thigh segment elevation angle is modified on a negative slope, whereas the shank elevation angle is modified on a positive slope (Fig. 2a). In both situations, the variability increases (Fig. 1b) and the range of motion decreases (Dewolf et al. 2018).

The variability of inter-segmental coordination (DP; Fig. 3) is significantly affected by slope and speed. Indeed, $DP_{thigh\text{-}shank}$ and $DP_{shank\text{-}foot}$ are greater at slow speeds and in downhill walking. A small variability during locomotion has been related to the capacity of maintaining dynamic balance (Buzzi and Ulrich 2004; Chiu and Chou 2012). On the contrary, a large variability has been associated with a lower ability to maintain balance, which in turn may increase the risk of falling (Chiu and Chou 2012, 2013; Yen et al. 2009). The large variability that we observed during slow downhill walking also suggests a more challenging task for the neuromuscular control (Hunter et al. 2010; Vieira et al. 2017).

When compared to level walking, muscular activities in the lower-limb also provide evidence that subjects slightly adjust their control strategies on slopes. At all slopes, the average FWHM across the 16 lower-limb muscles decreases when speed increases and, it is greater in downhill walking than on the level (Fig. 5b). The co-activation observed between agonist/antagonist muscles (Fig. 5c) is seen to increase in uphill walking and in slow downhill walking. While during downhill walking, this co- activation could potentially be due to an instability brought on by the negative slope (Sheehan and Gottschall 2012; Vieira et al. 2017), in uphill walking it is most likely due to a greater level of muscle activation. In turn, the greater co-activation may influence the cost of transportation and, consequently, the optimal walking speed (Gomeñuka et al. 2014, 2016).

The present analysis of muscle coordination using NNMF showed that four muscle synergies accounted for > 90% of variability in the EMG profiles at each walking condition, supporting the idea of a flexible use of fundamental synergies during slope and level walking (Janshen et al. 2017; Rozumalski et al. 2017; Saito et al. 2018). Although this "program" is rather invariant across speeds and slopes despite changes in the biomechanical task constraints, the amplitude of the basic activation patterns and the associated weighting coefficients (Fig. 6a) change with speed and slope. In particular, the amplitude of the second basic component P2, associated with the propulsion in late-stance (Neptune et al. 2009; Dewolf et al. 2019) increases during uphill but decreases during downhill walking (Fig. 6a). Moreover, the VAF by the first muscular pattern is much greater in downhill walking than in level and uphill walking (Fig. 6b). While the modifications of the neuromuscular pattern brought by the slope are most likely too subtle to induce significant modification of the number of basic activation patterns (Fig. 6b; Janshen et al. 2017; Rozumalski et al. 2017; Saito

et al. 2018), the VAF by only one synergy has been proposed as a potential metric to assess the complexity of motor control (Steele et al. 2015) and has been associated with clinical outcomes (Cruz-Montecinos et al. 2019). Therefore, the results of the present study may indirectly suggest that the complexity of motor control is reduced in downhill walking.

Another modification of the muscular coordination on slopes is the wider FWHM across the 4 basic patterns observed in downhill walking at slow speeds (Fig. 6c). The wider shape of muscle activities and basic activation patterns have already been associated with variability in motor control, as for example during walking and running on uneven terrain (Santuz et al. 2018, 2020), in patients with balance control disorder (Martino et al. 2015) or in children with cerebral palsy (Cappellini et al. 2016).

Our results also support the hypothesis of a speed-dependent control of locomotion (Biewener and Daley 2007; Dewolf et al. 2018; Full and Koditschek 1999; Yokoyama et al. 2016, 2017). Indeed, the similarities of associated weighting coefficients between slope and level walking are smaller at slow speeds (Fig. 6), especially on negative slopes. Similar trends are observed on kinematic coordination (Fig. 3; Dewolf et al. 2018). When walking slowly, the body centre of mass remains close to the polygon of support and the variability of the system is greater than at fast speeds, most likely because stability relies on a voluntary coordination of movement involving higher brain centers [sic] (Biewener and Daley 2007). As speed increases, the variability of the system decreases. Biewener and Daley (2007) hypothesised that the control of these fast movements depends more strongly on responses originated at more local levels [sic].

In summary, our findings suggest that the control strategy of downhill walking are similar to the more cautious gait pattern observed when stability is challenged (Santuz et al. 2018, 2020; Martino et al. 2015). Indeed, on a negative slope the stride width is wider, the variability of the stride period and of the inter-segmental coordination is greater and the basic activation patterns become broader. In such a challenging situation, this strategy may increase the ability to recover from perturbations of the system and may be adopted to lower the risk of falling at the cost of a greater energy consumption (Hunter et al. 2010; Monsch et al. 2012). On positive slopes, we found a greater variability of stride period and a greater stride width without temporal rearrangement of basic activation patterns and without modification of the variability of intersegmental coordination. In uphill walking where metabolic demands are high (Margaria 1968; Minetti et al. 1993), this strategy may be planned to make the minimisation of energy expenditure a priority.

Acknowledgements The authors would like to thank Pr. K. Zelik for his help during the experiment and the Pr. F. Lacquaniti and Dr. I. Ivanenko for their help in Formal analysis.

Author contributions Conceptualisation: PAW; Data curation: PAW; Formal analysis: AHD; Funding acquisition: PAW; Investigation: AHD; Methodology: AHD; Project administration: PAW; Software: AHD; Supervision: PAW; Writing—original draft: AHD; Writing—review and editing: AHD, RMM, PAW.

Funding This study was funded by the Universite catholique de Louvain (Belgium) and the Fonds de la Recherche Scientifique (Belgium).

Compliance with ethical standards

Conflict of interest The authors declare that the research was conducted in the absence of any commercial or financial relationships that could be construed as a potential conflict of interest.

References

Allen JL, Franz JR (2018) The motor repertoire of older adult fallers may constrain their response to balance perturbations. J Neurophysiol 120(5):2368–2378. https://doi.org/10.1152/jn.00302.2018

Baggen RJ, van Dieën JH, Van Roie E et al (2020) Age-related differences in muscle synergy organization during step ascent at different heights and directions. Appl Sci 10:1987. https://doi.org/10.3390/app10061987

Bernstein NA (1967) The Co-ordination and regulation of movements. Pergamon Press, Oxford

Bianchi L, Angelini D, Orani GP, Lacquaniti F (1998) Kinematic coordination in human gait: relation to mechanical energy cost. J Neurophysiol 79(4):2155–2170. https://doi.org/10.1152/jn.1998.79.4.2155

Biewener AA, Daley MA (2007) Unsteady locomotion: integrating muscle function with whole body dynamics and neuromuscular control. J Exp Biol 210(17):2949–2960. https://doi.org/10.1242/jeb.005801

Birn-Jeffery AV, Higham TE (2014) The scaling of uphill and downhill locomotion in legged animals. Integr Comp Biol 54(6):1159–1172. https://doi.org/10.1093/icb/icu015

Borghese NA, Bianchi L, Lacquaniti F (1996) Kinematic determinants of human locomotion. J Physiol 494(3):863–879. https://doi.org/10.1113/jphysiol.1996.sp021539

Buzzi UH, Ulrich BD (2004) Dynamic stability of gait cycles as a function of speed and system constraints. Mot Control 8(3):241–254. https://doi.org/10.1123/mcj.8.3.241

Byrne JE, Stergiou N, Blanke D, Houser JJ, Kurz MJ, Hageman PA (2002) Comparison of gait patterns between young and elderly women: an examination of coordination. Percept Mot Skills 94(1):265–280. https://doi.org/10.2466/pms.2002.94.1.265

Cappellini G, Ivanenko YP, Martino G, MacLellan MJ, Sacco A, Morelli D, Lacquaniti F (2016) Immature spinal locomotor output in children with cerebral palsy. Front Physiol. https://doi.org/10.3389/fphys.2016.00478

Catavitello G, Ivanenko YP, Lacquaniti F (2018) A kinematic synergy for terrestrial locomotion shared by mammals and birds. eLife 7:1–28. https://doi.org/10.7554/eLife.38190

Cheung VCK, D'Avella A, Tresch MC, Bizzi E (2005) Central and sensory contributions to the activation and organization of muscle synergies during natural motor behaviors. J Neurosci 25(27):6419–6434. https://doi.org/10.1523/JNEUROSCI.4904-04.2005

Cheung VCK, Turolla A, Agostini M, Silvoni S, Bennis C, Kasi P, Bizzi E (2012) Muscle synergy patterns as physiological markers of

motor cortical damage. Proc Natl Acad Sci USA 109(36):14652–14656. https://doi.org/10.1073/pnas.1212056109

Chiu S-L, Chou L-S (2012) Effect of walking speed on inter-joint coordination differs between young and elderly adults. J Biomech 45(2):275–280. https://doi.org/10.1016/j.jbiomech.2011.10.028

Chiu S-L, Chou L-S (2013) Variability in inter-joint coordination during walking of elderly adults and its association with clinical balance measures. Clin Biomech 28(4):454–458. https://doi.org/10.1016/j.clinbiomech.2013.03.001

Clark DJ, Ting LH, Zajac FE, Neptune RR, Kautz SA (2010) Merging of healthy motor modules predicts reduced locomotor performance and muscle coordination complexity post-stroke. J Neurophysiol 103(2):844–857. https://doi.org/10.1152/jn.00825.2009

Cruz-Montecinos C, Pérez-Alenda S, Cerda M, Maas H (2019) Neuromuscular control during gait in people with haemophilic arthropathy. Haemophilia 25:e69–e77. https://doi.org/10.1111/hae.13697

da Rosa RG, Gomeñuka NA, de Oliveira HB, Peyré-Tartaruga LA (2018) Inclined weight-loaded walking at different speeds: pelvis-shoulder coordination, trunk movements and cost of transport. J Mot Behav 50:73–79. https://doi.org/10.1080/00222895.2017.1283292

Dewolf AH, Peñailillo LE, Willems PA (2016) The rebound of the body during uphill and downhill running at different speeds. J Exp Biol 219:2276–2288. https://doi.org/10.1242/jeb.142976

Dewolf AH, Ivanenko YP, Lacquaniti F, Willems PA (2017) Pendular energy transduction within the step during human walking on slopes at different speeds. PLoS ONE. https://doi.org/10.1371/journal.pone.0186963

Dewolf AH, Ivanenko YP, Zelik KE, Lacquaniti F, Willems PA (2018) Kinematic patterns while walking on a slope at different speeds. J Appl Physiol 125(2):642–653. https://doi.org/10.1152/japplphysiol.01020.2017

Dewolf AH, Ivanenko Y, Zelik KE, Lacquaniti F, Willems PA (2019) Differential activation of lumbar and sacral motor pools during walking at different speeds and slopes. J Neurophysiol. https://doi.org/10.1152/jn.00167.2019

Dominici N, Ivanenko YP, Cappellini G, Zampagni ML, Lacquaniti F (2010) Kinematic strategies in newly walking toddlers stepping over different support surfaces. J Neurophysiol 103(3):1673–1684. https://doi.org/10.1152/jn.00945.2009

Dominici N, Ivanenko YP, Cappellini G, D'Avella A, Mondì V, Cicchese M, Lacquaniti F (2011) Locomotor primitives in newborn babies and their development. Science 334(6058):997–999. https://doi.org/10.1126/science.1210617

Ferraro RA, Pinto-Zipp G, Simpkins S, Clark MA (2013) Effects of an inclined walking surface and balance abilities on spatiotemporal gait parameters of older adults. J Geriatr Phys Ther 36(1):31–38. https://doi.org/10.1519/JPT.0b013e3182510339

Full RJ, Koditschek DE (1999) Templates and anchors: neuromechanical hypotheses of legged locomotion on land. J Exp Biol 202(23):3325–3332

Gambelli CN, Theisen D, Willems PA, Schepens B (2016) Motor control of landing from a countermovement jump in simulated microgravity. J Appl Physiol 120:1230–1240. https://doi.org/10.1152/japplphysiol.00993.2015

Gizzi L, Nielsen JF, Felici F, Ivanenko YP, Farina D (2011) Impulses of activation but not motor modules are preserved in the locomotion of subacute stroke patients. J Neurophysiol 106(1):202–210. https://doi.org/10.1152/jn.00727.2010

Gomeñuka NA, Bona RL, da Rosa RG, Peyré-Tartaruga LA (2014) Adaptations to changing speed, load, and gradient in human walking: cost of transport, optimal speed, and pendulum. Scand J Med Sci Sports 24:e165–173. https://doi.org/10.1111/sms.12129

Gomeñuka NA, Bona RL, da Rosa RG, Peyré-Tartaruga LA (2016) The pendular mechanism does not determine the optimal speed of loaded walking on gradients. Hum Mov Sci 47:175–185. https://doi.org/10.1016/j.humov.2016.03.008

Gottschall JS, Kram R (2006) Mechanical energy fluctuations during hill walking: the effects of slope on inverted pendulum exchange. J Exp Biol 209:4895–4900. https://doi.org/10.1242/jeb.02584

Grasso R, Zago M, Lacquaniti F (2000) Interactions between posture and locomotion: Motor patterns in humans walking with bent posture versus erect posture. J Neurophysiol 83(1):288–300. **(Retrieved from Scopus)**

Hak L, Houdijk H, Steenbrink F, Mert A, Van der Wurff P, Beek PJ, Van Dieën JH (2012) Speeding up or slowing down?: Gait adaptations to preserve gait stability in response to balance perturbations. Gait Posture 36(2):260–264. https://doi.org/10.1016/j.gaitpost.2012.03.005

Hausdorff JM (2007) Gait dynamics, fractals and falls: finding meaning in the stride-to-stride fluctuations of human walking. Hum Mov Sci 26(4):555–589. https://doi.org/10.1016/j.humov.2007.05.003

Hausdorff JM, Rios DA, Edelberg HK (2001) Gait variability and fall risk in community-living older adults: a 1-year prospective study. Arch Phys Med Rehabil 82(8):1050–1056. https://doi.org/10.1053/apmr.2001.24893

Hunter LC, Hendrix EC, Dean JC (2010) The cost of walking downhill: Is the preferred gait energetically optimal? J Biomech 43(10):1910–1915. https://doi.org/10.1016/j.jbiomech.2010.03.030

Ivanenko YP, Poppele RE, Lacquaniti F (2004) Five basic muscle activation patterns account for muscle activity during human locomotion. J Physiol 556(1):267–282. https://doi.org/10.1113/jphysiol.2003.057174

Ivanenko YP, Cappellini G, Dominici N, Poppele RE, Lacquaniti F (2005) Coordination of locomotion with voluntary movements in humans. J Neurosci 25(31):7238–7253. https://doi.org/10.1523/JNEUROSCI.1327-05.2005

Ivanenko YP, Poppele RE, Lacquaniti F (2006) Spinal cord maps of spatiotemporal alpha-motoneuron activation in humans walking at different speeds. J Neurophysiol 95(2):602–618. https://doi.org/10.1152/jn.00767.2005

Ivanenko YP, Cappellini G, Dominici N, Poppele RE, Lacquaniti F (2007) Modular control of limb movements during human locomotion. J Neurosci 27:11149–11161. https://doi.org/10.1523/JNEUROSCI.2644-07.2007

Janshen L, Santuz A, Ekizos A, Arampatzis A (2017) Modular control during incline and level walking in humans. J Exp Biol 220(Pt 5):807–813. https://doi.org/10.1242/jeb.148957

Kendall F, McCreary E, Provance P, Rodgers M, Romani W (2005) Muscles: testing and function with posture and pain, 5th edn. Lippincott Williams and Wilkins, Baltimore, MD

Lay AN, Hass CJ, Gregor RJ (2006) The effects of sloped surfaces on locomotion: a kinematic and kinetic analysis. J Biomech 39(9):1621–1628. https://doi.org/10.1016/j.jbiomech.2005.05.005

Lay AN, Hass CJ, Richard Nichols T, Gregor RJ (2007) The effects of sloped surfaces on locomotion: an electromyographic analysis. J Biomech 40(6):1276–1285. https://doi.org/10.1016/j.jbiomech.2006.05.023

Lee DD, Seung HS (2001) Algorithms for non-negative matrix factorization. Presented at the Advances in Neural Information Processing Systems. Retrieved from https://www.scopus.com/inward/record.uri?eid=2-s2.0-84898964201&partnerID=40&md5=d1974c80e29ec37759872f4a8ce6d823. Accessed 7 June 2020

Leroux A, Fung J, Barbeau H (2002) Postural adaptation to walking on inclined surfaces: I. Normal strategies. Gait Posture 15(1):64–74. https://doi.org/10.1016/S0966-6362(01)00181-3

Maki BE (1997) Gait changes in older adults: predictors of falls or indicators of fear? J Am Geriatr Soc 45(3):313–320. https://doi.org/10.1111/j.1532-5415.1997.tb00946.x

Margaria R (1968) Positive and negative work performances and their efficiencies in human locomotion. Int Z Angew Physiol Einschl Arbeitsphysiol 25(4):339–351. https://doi.org/10.1007/BF00699624

Mari S, Serrao M, Casali C, Conte C, Martino G, Ranavolo A, Pierelli F (2014) Lower limb antagonist muscle co-activation and its relationship with gait parameters in cerebellar ataxia. Cerebellum 13(2):226–236. https://doi.org/10.1007/s12311-013-0533-4

Martino G, Ivanenko YP, Serrao M, Ranavolo A, d'Avella A, Draicchio F, Lacquaniti F (2014) Locomotor patterns in cerebellar ataxia. J Neurophysiol 112(11):2810–2821. https://doi.org/10.1152/jn.00275.2014

Martino G, Ivanenko YP, d'Avella A, Serrao M, Ranavolo A, Draicchio F, Lacquaniti F (2015) Neuromuscular adjustments of gait associated with unstable conditions. J Neurophysiol 114(5):2867–2882. https://doi.org/10.1152/jn.00029.2015

McAndrew PM, Dingwell JB, Wilken JM (2010) Walking variability during continuous pseudo-random oscillations of the support surface and visual field. J Biomech 43(8):1470–1475. https://doi.org/10.1016/j.jbiomech.2010.02.003

McIntosh AS, Beatty KT, Dwan LN, Vickers DR (2006) Gait dynamics on an inclined walkway. J Biomech 39(13):2491–2502. https://doi.org/10.1016/j.jbiomech.2005.07.025

Minetti AE, Ardigò LP, Saibene F (1993) Mechanical determinants of gradient walking energetics in man. J Physiol 472(1):725–735. https://doi.org/10.1113/jphysiol.1993.sp019969

Monaco V, Ghionzoli A, Micera S (2010) Age-related modifications of muscle synergies and spinal cord activity during locomotion. J Neurophysiol 104(4):2092–2102. https://doi.org/10.1152/jn.00525.2009

Monsch ED, Franz CO, Dean JC (2012) The effects of gait strategy on metabolic rate and indicators of stability during downhill walking. J Biomech 45(11):1928–1933. https://doi.org/10.1016/j.jbiomech.2012.05.024

Neptune RR, Clark DJ, Kautz SA (2009) Modular control of human walking: a simulation study. J Biomech 42:1282–1287. https://doi.org/10.1016/j.jbiomech.2009.03.009

Noble JW, Prentice SD (2008) Intersegmental coordination while walking up inclined surfaces: age and ramp angle effects. Exp Brain Res 189(2):249–255. https://doi.org/10.1007/s00221-008-1464-z

Ogaya S, Iwata A, Higuchi Y, Fuchioka S (2016) The association between intersegmental coordination in the lower limb and gait speed in elderly females. Gait Posture 48:1–5. https://doi.org/10.1016/j.gaitpost.2016.04.018

Peyré-Tartaruga LA, Coertjens M (2018) Locomotion as a powerful model to study integrative physiology: efficiency, economy, and power relationship. Front Physiol. https://doi.org/10.3389/fphys.2018.01789

Pickle NT, Grabowski AM, Auyang AG, Silverman AK (2016) The functional roles of muscles during sloped walking. J Biomech 49(14):3244–3251. https://doi.org/10.1016/j.jbiomech.2016.08.004

Prentice SD, Hasler EN, Groves JJ, Frank JS (2004) Locomotor adaptations for changes in the slope of the walking surface. Gait Posture 20(3):255–265. https://doi.org/10.1016/j.gaitpost.2003.09.006

Ranavolo A, Donini LM, Mari S, Serrao M, Silvetti A, Iavicoli S, Draicchio F (2013) Lower-limb joint coordination pattern in obese subjects. Biomed Res Int. https://doi.org/10.1155/2013/142323

Rozumalski A, Steele KM, Schwartz MH (2017) Muscle synergies are similar when typically developing children walk on a treadmill at different speeds and slopes. J Biomech 64:112–119. https://doi.org/10.1016/j.jbiomech.2017.09.002

Rudolph KS, Axe MJ, Snyder-Mackler L (2000) Dynamic stability after ACL injury: who can hop? Knee Surg Sports Traumatol Arthrosc 8:262–269

Saito A, Tomita A, Ando R, Watanabe K, Akima H (2018) Similarity of muscle synergies extracted from the lower limb including the deep muscles between level and uphill treadmill walking. Gait Posture 59:134–139. https://doi.org/10.1016/j.gaitpost.2017.10.007

Santuz A, Ekizos A, Eckardt N, Kibele A, Arampatzis A (2018) Challenging human locomotion: stability and modular organisation in unsteady conditions. Sci Rep. https://doi.org/10.1038/s41598-018-21018-4

Santuz A, Brüll L, Ekizos A et al (2020) Neuromotor dynamics of human locomotion in challenging settings. iScience 23:100796. https://doi.org/10.1016/j.isci.2019.100796

Sartori M, Gizzi L, Lloyd DG, Farina D (2013) A musculoskeletal model of human locomotion driven by a low dimensional set of impulsive excitation primitives. Front Comput Neurosci (JUN). https://doi.org/10.3389/fncom.2013.00079

Sheehan RC, Gottschall JS (2012) At similar angles, slope walking has a greater fall risk than stair walking. Appl Ergon 43(3):473–478. https://doi.org/10.1016/j.apergo.2011.07.004

Steele KM, Rozumalski A, Schwartz MH (2015) Muscle synergies and complexity of neuromuscular control during gait in cerebral palsy. Dev Med Child Neurol 57(12):1176–1182. https://doi.org/10.1111/dmcn.12826

Stergiou N, Scholten SD, Jensen JL, Blanke D (2001) Intralimb coordination following obstacle clearance during running: the effect of obstacle height. Gait Posture 13(3):210–220. https://doi.org/10.1016/S0966-6362(00)00101-6

Torres-Oviedo G, Ting LH (2007) Muscle synergies characterizing human postural responses. J Neurophysiol 98:2144–2156. https://doi.org/10.1152/jn.01360.2006

Torres-Oviedo G, Macpherson JM, Ting LH (2006) Muscle synergy organization is robust across a variety of postural perturbations. J Neurophysiol 96(3):1530–1546. https://doi.org/10.1152/jn.00810.2005

Van Emmerik REA, Wagenaar RC (1996) Effects of walking velocity on relative phase dynamics in the trunk in human walking. J Biomech 29(9):1175–1184. https://doi.org/10.1016/0021-9290(95)00128-X

Vieira MF, Rodrigues FB, de Sá e Souza GS, Magnani RM, Lehnen GC, Campos NG, Andrade AO (2017) Gait stability, variability and complexity on inclined surfaces. J Biomech 54:73–79. https://doi.org/10.1016/j.jbiomech.2017.01.045

Winter DA (1991) The biomechanics and motor control of human gait: normal, elderly and pathological. Waterloo Biomechanics, Waterloo

Winter DA (1992) Foot trajectory in human gait: a precise and multifactorial motor control task. Phys Ther 72(1):45–56. **(Retrieved from Scopus)**

Xu H, Wang Y, Greenland K, Bloswick D, Merryweather A (2015) The influence of deformation height on estimating the center of pressure during level and cross-slope walking on sand. Gait Posture 42(2):110–115. https://doi.org/10.1016/j.gaitpost.2015.04.015

Yen H-C, Chen H-L, Liu M-W, Liu H-C, Lu T-W (2009) Age effects on the inter-joint coordination during obstacle-crossing. J Biomech 42(15):2501–2506. https://doi.org/10.1016/j.jbiomech.2009.07.015

Yokoyama H, Ogawa T, Kawashima N, Shinya M, Nakazawa K (2016) Distinct sets of locomotor modules control the speed and modes of human locomotion. Sci Rep. https://doi.org/10.1038/srep36275

Yokoyama H, Ogawa T, Shinya M, Kawashima N, Nakazawa K (2017) Speed dependency in α-motoneuron activity and locomotor modules in human locomotion: indirect evidence for phylogenetically conserved spinal circuits. Proc R Soc B Biol Sci. https://doi.org/10.1098/rspb.2017.0290